metals

MDPI

Article

Enhanced Mechanical Properties of MgZnCa Bulk Metallic Glass Composites with Ti-Particle Dispersion

Pei Chun Wong [1], Tsung Hsiung Lee [2], Pei Hua Tsai [2], Cheng Kung Cheng [1,*], Chuan Li [1], Jason Shian-Ching Jang [2,3,*] and J. C. Huang [4]

1 Department of Biomedical Engineering, National Yang-Ming University, Taipei 11221, Taiwan; s0925135546@gmail.com (P.C.W.); cli10@ym.edu.tw (C.L.)
2 Institute of Materials Science and Engineering, National Central University, Taoyuan 32001, Taiwan; pshunterbabu@gmail.com (T.H.L.); peggyphtsai@gmail.com (P.H.T.)
3 Department of Mechanical Engineering, National Central University, Taoyuan 32001, Taiwan
4 Department of Materials and Optoelectronic Science, National Sun Yat-Sen University, Kaohsiung 80424, Taiwan; jacobc@mail.nsysu.edu.tw
* Correspondence: ckcheng@ym.edu.tw (C.K.C.); jscjang@ncu.edu.tw (J.S.C.J.); Tel.: +886-2-2826-7020 (C.K.C.); +886-3-426-7379 (J.S.C.J.); Fax: +886-2-2822-8557 (C.K.C.); +886-3-425-4501 (J.S.C.J.)

Academic Editor: Ana Sofia Ramos
Received: 16 February 2016; Accepted: 10 May 2016; Published: 17 May 2016

Abstract: Rod samples of $Mg_{60}Zn_{35}Ca_5$ bulk metallic glass composites (BMGCs) dispersed with Ti particles have been successfully fabricated via injection casting. The glass forming ability (GFA) and the mechanical properties of these Mg-based BMGCs have been systematically investigated as a function of the volume fraction (V_f) of Ti particles. The results showed that the compressive ductility increased with V_f. The mechanical performance of these BMGCs, with up to 5.4% compressive failure strain and 1187 MPa fracture strength at room temperature, can be obtained for the Mg-based BMGCs with 50 vol % Ti particles, suggesting that these dispersed Ti particles can absorb the energy of the crack propagations and can induce branches of the primary shear band into multiple secondary shear bands. It follows that further propagation of the shear band is blocked, enhancing the overall plasticity.

Keywords: composite; Mg-Zn-Ca; bulk metallic glass; self-degraded ability; mechanical properties

1. Introduction

Organ protection, muscle connection, and muscle action promotion are the most important functions of bone [1]. Once the bone is fractured due to impact or other external forces during, for example, sports activities or accidents, it needs to be reconstructed to recover its normal function. Therefore, bone screws, bone plates, and bone substitute materials are usually applied to fixate the fractured bones via medical surgery. In general, austenitic stainless steel, Co–Cr alloys, and Ti alloys have been commercially used in orthopedic implants, taking advantage of their good mechanical properties, biocompatibility, and corrosion resistance. However, most metallic orthopedic implant metals (except Ti alloys) are potentially cytotoxic when the implant parts are retained in the body for long periods of time. Therefore, medical doctors may suggest that the patient undergo a second operation to take out the old prosthesis and to replace a new one. Accordingly, to avoid secondary surgery and reduce surgical risk, biodegradable materials have become a trend for biomaterials development. Metallic biodegradable materials have attracted great attention because of their promising mechanical properties, good biocompatibility, and low degradation rate. The metallic biodegradable materials, including W-based, Ca-based, Fe-based, Zn-based, and Mg-based alloys,

have been wildly studied for their physical properties, chemical properties, and their biocompatibility in the last decade.

Among these metallic biodegradable materials, Mg-based alloys have attracted more attention as biomedical materials because of their good biocompatibility and appropriate biodegradability. In parallel, the strength and Young's modulus of Mg-based alloys are closer to those of bone tissue, reducing the stress shielding effect. Though the Mg-based materials have great potential for applications on many biomedical instruments and orthopedic implants, the corrosion and degradation rates of most Mg-based crystalline alloys are still too fast. Conversely, MgZnCa bulk metallic glass composites (BMGCs) were found to present much lower corrosion rates than the other Mg-based crystalline alloys. Unfortunately, monolithic MgZnCa bulk metallic glasses are quite brittle, limiting their further applications [2–6]. There have hitherto been a number of studies reporting on effective methods that enhance the strength as well as the plasticity of Mg-based BMGCs through the dispersion of ductile metallic particles such as those of Mo, Fe, Nb, and Ti [7–17]. These ductile metallic particles can absorb the shear strain energy of shear bands, confine the propagation of shear bands, and significantly improve their plasticity. In this study, Ti particles were selected to add to the MgZnCa metallic glasses to improve their plasticity because Ti metal is well-known for having non-toxicity, good biocompatibility, and an immiscible reaction with the parent Mg metal.

2. Experimental

$Mg_{60}Zn_{35}Ca_5$-based BMGCs with different volume fractions of Ti particles (V_f = 20, 30, 40, and 50 vol %) were prepared by induction melting under an argon atmosphere. At first, high purity Mg, Zn, Ca (>99.9%), and pure Ti particles (three distributions in diameters, namely, 20–75, 75–105 and 105–130 μm) were melted together by induction melting under the argon atmosphere. During melting, the melt was churned mechanically to assure a final ingot containing a homogeneous mixture of Ti particles and melt. The $Mg_{60}Zn_{35}Ca_5$–Ti composite ingot was re-melted in a quartz tube and injected into a water-cooled Cu mold by argon pressure to form Mg-based BMGC rods, measuring 20 mm in length and 2 mm in diameter.

The amorphous state of $Mg_{60}Zn_{35}Ca_5$-BMGCs was examined by X-ray diffraction (XRD, Shimadzu XRD6000, Shimadzu Corporation, Kyoto, Japan) with monochromatic Cu–Kα radiation. The chemical compositions of samples were verified by energy dispersive spectroscopy (EDS, FEI, Quanta 3D FEG, FEI Corporation, Hillsboro, OR, USA) to confirm their compositions as the original design. The thermal properties were analyzed by differential scanning calorimetry (DSC, Mettler DSC1, Mettler-Toledo International Inc, Greifensee, Switzerland) under an argon atmosphere at a heating rate of 40 K/min. The DSC results were then used to calculate the glass forming ability (GFA). The uniaxial compression tests were carried out by a universal test system (Hung Ta, HT9102, Taipei, Taiwan) at a strain rate of 1×10^{-4} s^{-1}. The specimens were cut from the as-cast rods into compression test specimens measuring 4 mm in length and 2 mm in diameter. The latter specimens were polished for both ends to confirm the surface flatness. The tests of hardness and fracture toughness (K_C, stress concentration factor) for all Mg-based BMGCs were carried out via the indentation method [18] with a microhardness tester (Mitutoyo, HM-221, Kanagawa, Japan) with a load of 1–2 kgf. Both the surface morphology and fractography of compressed specimens were examined by scanning electron microscopy (SEM. FEI Quanta 3D FEG).

3. Result and Discussion

The XRD patterns of the $Mg_{60}Zn_{35}Ca_5$ base alloy, $Mg_{60}Zn_{35}Ca_5$-based BMGCs with 50 vol % Ti particles, and pure Ti particles are shown in Figure 1. Both XRD patterns of the base alloy with and without Ti particles show an amorphous nature with a broadened diffuse hump, except for several peaks from the crystalline Ti particles co-existing in the XRD pattern of the composite sample. Some of the crystalline peaks were quite unclear because of another phase precipitated out around the Ti particles, as shown in Figure 2.

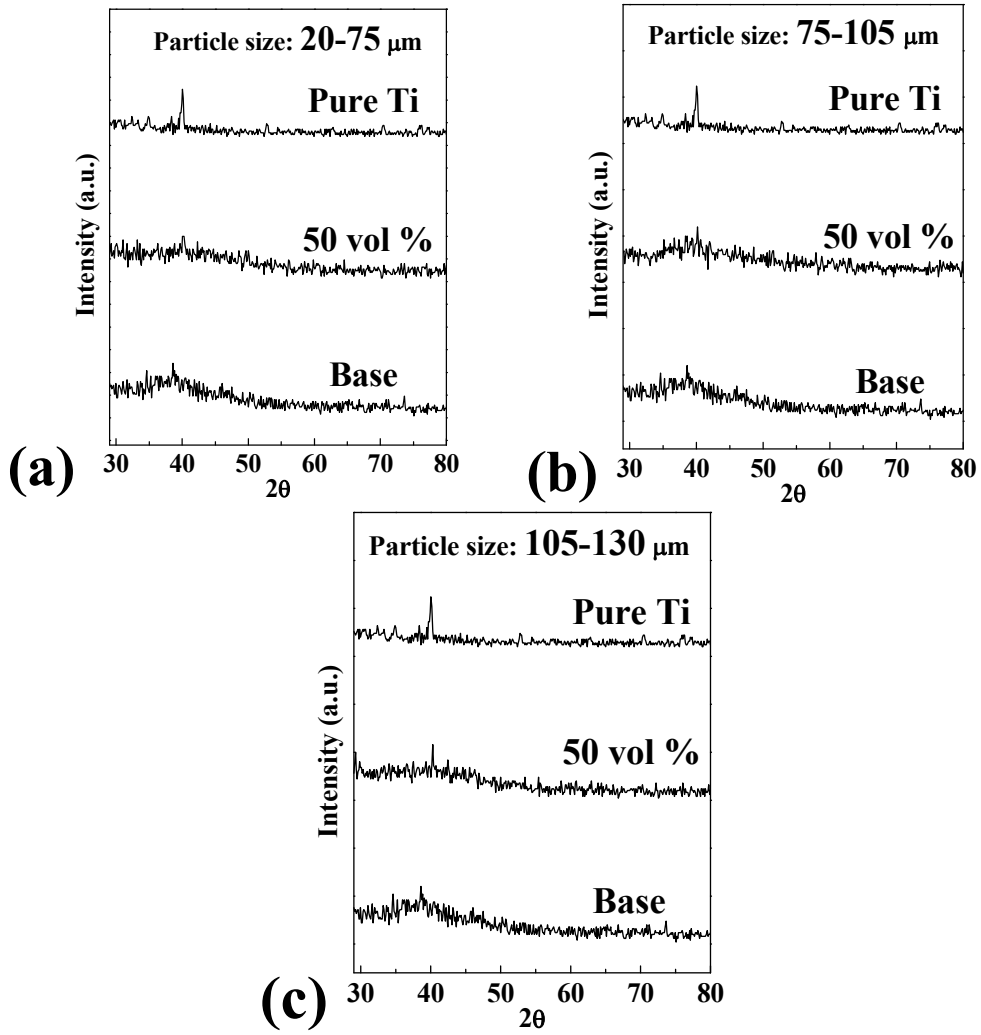

Figure 1. X-ray diffraction (XRD) pattern of the pure Ti particle, $Mg_{60}Zn_{35}Ca_5$ base alloy, and $Mg_{60}Zn_{35}Ca_5$-based bulk metallic glass composites (BMGCs) containing 50 vol % Ti particles with different particle sizes of (**a**) 20–75 μm; (**b**) 75–105 μm; (**c**) 105–130 μm.

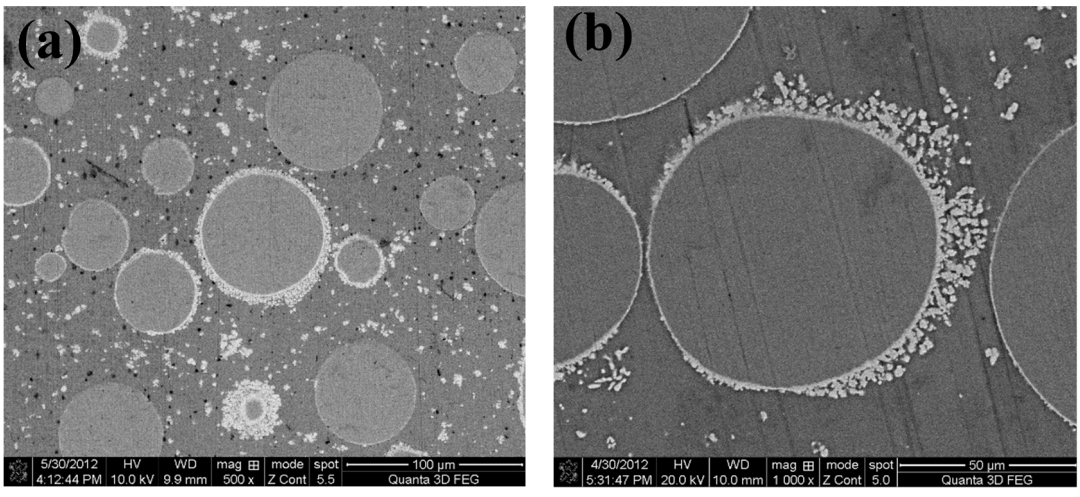

Figure 2. *Cont.*

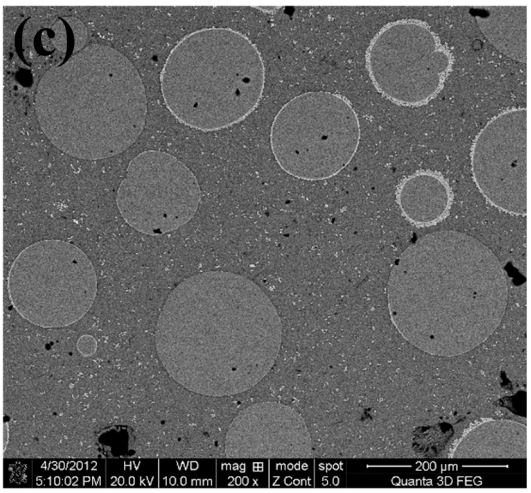

Figure 2. Back-scattering electron images of $Mg_{60}Zn_{35}Ca_5$-based BMGC samples containing different particle size of 50 vol % Ti particles: (**a**) 20–75 µm; (**b**) 75–105 µm; and (**c**) 105–130 µm.

The representative DSC scans of the $Mg_{60}Zn_{35}Ca_5$-based BMGCs with different volume fractions of 75–105 µm Ti particles are shown in Figure 3. Regardless of the inserted Ti particle size, both the glass transition temperature (T_g) and crystallization temperature (T_x) of $Mg_{60}Zn_{35}Ca_5$-based BMGCs exhibit a decreasing trend with an increasing volume fraction of Ti particles. This result indicates that both the glass transition and crystallization were trigged earlier by the presence of a large amount of crystalline Ti particles. The mechanism of such changes might be attributed to the numerous increases of heterogeneous nucleation sites from the interfaces between the Mg-based amorphous matrix and Ti particles. In addition, the calculated GFA indices were also found to decrease with an increasing volume fraction of Ti particles as shown in Table 1, supporting the mentioned mechanism of a lowering reaction barrier for crystallization.

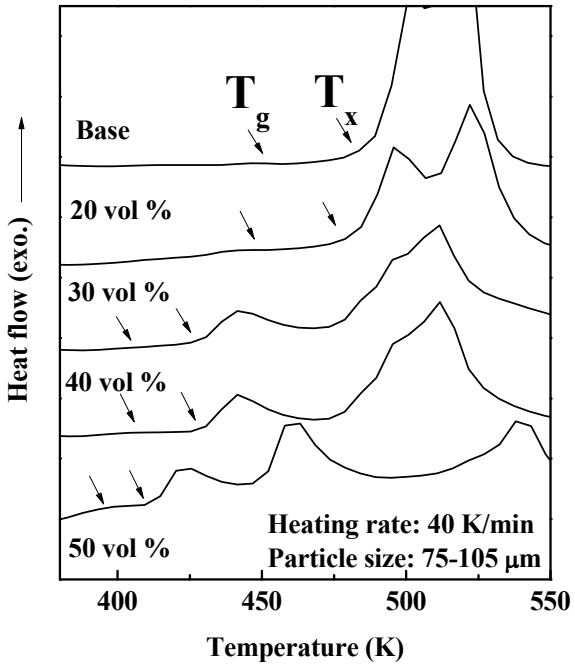

Figure 3. Representative differential scanning calorimetry (DSC) scans of $Mg_{60}Zn_{35}Ca_5$-based BMGC samples containing different volume fractions of 75–105-µm-sized Ti particles.

Table 1. Glass forming ability of $Mg_{60}Zn_{35}Ca_5$base alloy and $Mg_{60}Zn_{35}Ca_5$-based BMGCs.

Particle Size (D)	vol %	T_g (K)	T_x (K)	T_l (K)	T_{rg}	γ	γ_m	ΔT_x
Base		446	488	700	0.638	0.426	0.758	42
20–75 μm	20	400	430	675	0.593	0.400	0.681	30
	30	400	429	671	0.597	0.400	0.683	29
	40	403	432	674	0.598	0.401	0.684	29
	50	395	418	676	0.585	0.391	0.654	23
75–105 μm	20	394	433	679	0.580	0.404	0.698	40
	30	402	430	673	0.599	0.400	0.681	28
	40	404	429	672	0.601	0.399	0.677	25
	50	393	414	673	0.584	0.388	0.646	21
105–130 μm	20	408	435	671	0.609	0.403	0.688	27
	30	405	431	681	0.595	0.396	0.670	25
	40	400	425	680	0.588	0.394	0.663	25
	50	400	425	682	0.587	0.392	0.658	24

$T_{rg} = \frac{T_g}{T_l}; \gamma = \frac{T_x}{T_g+T_l}; \gamma_m = \frac{2T_x-T_g}{T_l}$.

Some representative back-scattering SEM images of the Mg-based BMGCs containing different sizes and a fixed volume fraction of Ti particles are shown in Figure 2. At a fixed volume fraction of Ti particles, the average inter-particle space of Ti particles clearly shows a decreasing trend with a decreasing size of Ti particles in the $Mg_{60}Zn_{35}Ca_5$-based BMGCs. The numerical values of inter-particle space of Ti particles for various combinations of particle size and volume fraction are summarized in Table 2. In addition, an extra phase was found to precipitate along the interface of the Ti particle/amorphous matrix around some Ti particles. These precipitates around the Ti particles were identified to be the TiZn compound based on its chemical composition (Ti: 52 atom %/Zn 48 atom %) analyzed by energy dispersive spectroscopy.

Table 2. Inter-particle spacing of $Mg_{60}Zn_{35}Ca_5$-based BMGCs.

Particle Size (D)	vol %	Inter-Particle Spacing (Edge to Edge, μm)	
		Calculated	Measured
20–75 μm (Average 48 μm)	20	59	53 ± 11
	30	40	42 ± 7
	40	28	36 ± 8
	50	18	19 ± 3
75–105 μm (Average 90 μm)	20	110	91 ± 21
	30	74	74 ± 14
	40	52	68 ± 12
	50	37	34 ± 4
105–130 μm (Average 120 μm)	20	148	135 ± 26
	30	99	117 ± 21
	40	68	83 ± 26
	50	50	65 ± 11

Figure 4 shows the compression stress–strain curves for the $Mg_{60}Zn_{35}Ca_5$-based BMGC samples (V_f = 20, 30, 40 and 50 vol %) tested at a strain rate of 1×10^{-4} s^{-1} at room temperature. The results show that the *ex-situ*-added Ti particles exhibit a positive effect on strengthening the $Mg_{60}Zn_{35}Ca_5$-based BMG. For the base Mg-based BMG, it only shows a compression strength of 655 MPa with a brittle fracture mode. On the contrary, the fracture strength level of $Mg_{60}Zn_{35}Ca_5$-based BMGCs was significantly increased by increasing the volume fraction of *ex situ*-added Ti particles. The fracture strength can reach 1190 MPa for the Mg-based BMGC with 50 vol % 20–75 μm Ti particles.

However, most BMGCs only show low failure strains, less than 3%. The brittle behavior of all Mg-based BMGC samples are presumed due to the brittle TiZn intermetallic compound that forms around the interface of the Ti particle/amorphous matrix and embrittle the Mg-based BMGC samples. Therefore, it is suggested that the Ti dispersoids cannot entirely restrict the propagation of the shear band due to its weak interface adhesion to the matrix. This can be evidenced from Figure 6, in which Ti particles were sheared apart from the matrix.

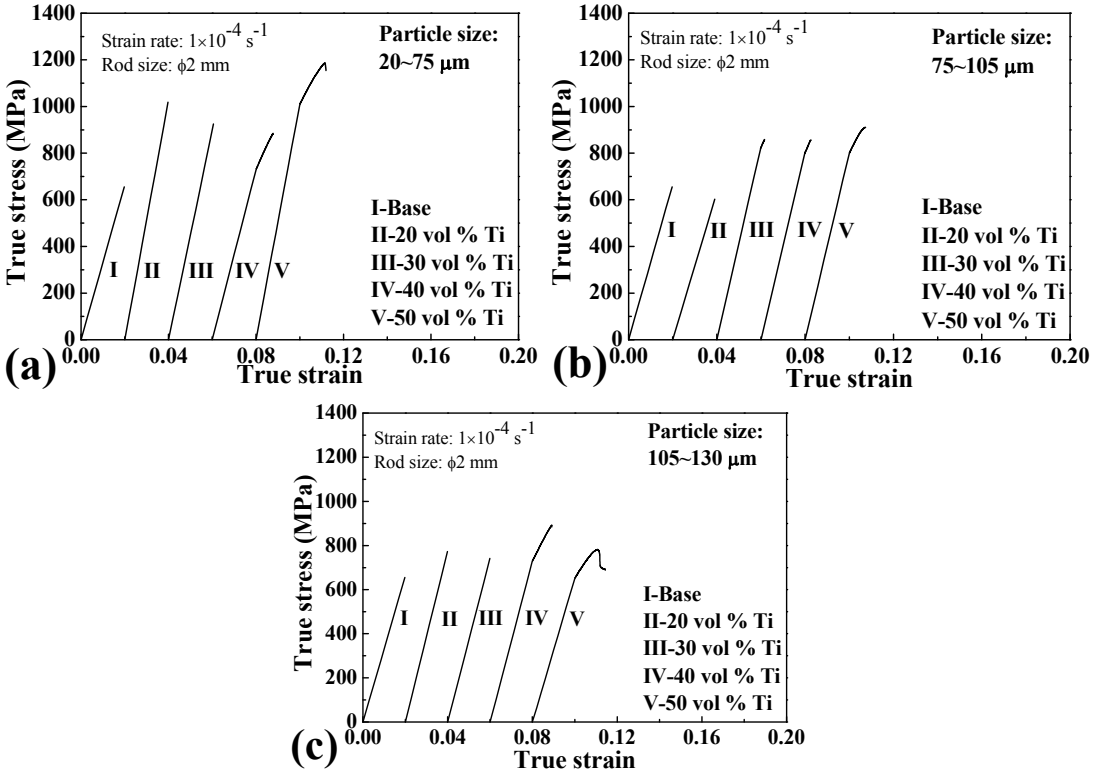

Figure 4. True stress–strain curve of $Mg_{60}Zn_{35}Ca_5$ BMGC rods containing different volume fractions and particles sizes of the Ti particles: (**a**) 20–75 μm; (**b**) 75–105 μm; (**c**) 105–130 μm.

The *ex situ* method may be a good possible way to enhance the plasticity of Mg-based BMGCs. In previous studies, the energy of the shear band can be absorbed by the dispersed particles (such as Fe, Mo, Ti, or Nb particles) in the Mg-based amorphous matrix alloys, and the shear band cannot easily propagate across the particles, significantly enhancing the plasticity of Mg-based BMGCs. Therefore, the combination of the large volume fraction and small particle size would create small inter-particle spacing of the dispersion phase to confine the propagation of shear bands and avoid the materials failure [15,18]. However, this theory does not seem to be applicable in every situation. In this study, the Mg-based BMGC samples with a smaller dispersoid size (20–75 μm) would present a lower failure strain than the Mg-based BMGC samples with a larger dispersoid size (75–105 μm). The reason is postulated to be a result of the brittle TiZn intermetallic compound precipitated out along the interface of the Ti particle/amorphous matrix, deteriorating the adhesion between the Ti particle and the amorphous matrix. Under the same volume fractions of the particles, the smaller particle size would create more interface areas of the Ti particle/amorphous matrix. Therefore, the interface of the Ti particle/amorphous matrix becomes a critical position of the crack initiation, leading to lower plastic deformation.

The dependency of the stress concentration factor (*Kc*) [19] and compression strain as a function of the interspacing of Ti particles for the Mg-based BMGCs is presented in Figure 5. Both the fracture toughness and the compression failure strain show a similar trend; they increase with a decreasing

interspacing of Ti particles, the mean free path of the shear band. It is apparent that the mean free path plays an important role in enhancing the toughness of $Mg_{60}Zn_{35}Ca_5$-based BMGCs.

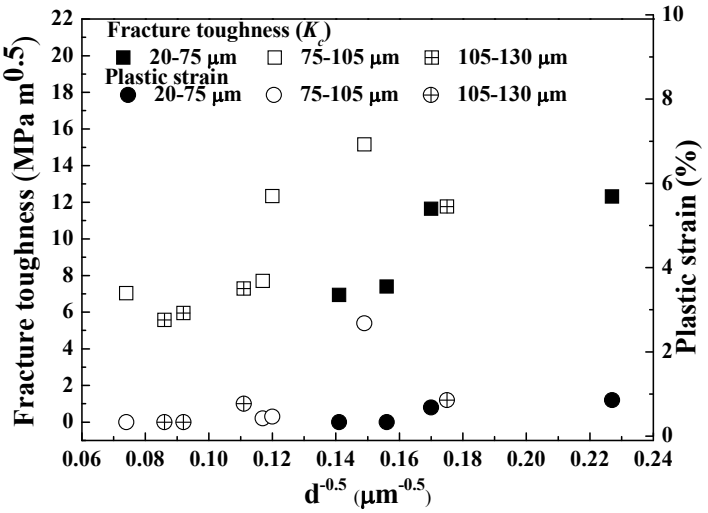

Figure 5. K_c (stress concentration factor) and compressive plastic strain as a function of the interspacing of various Ti particle additions of the $Mg_{60}Zn_{35}Ca_5$ BMGC rods with 2 mm in diameter.

The fracture surface of these $Mg_{60}Zn_{35}Ca_5$-based BMGC samples after the compression test exhibits two kinds of morphology. One is the rough fracture surface with a vein pattern and the other is the wavy surface with plastically sheared Ti particles, as shown in Figure 6. Figure 6a shows the relatively homogeneous distributed Ti particles on the fracture surface of Mg-based BMGC samples. Some Ti particles were peeled off from the matrix, implying a weak adhesion of some interfaces of the Ti particle/amorphous matrix. In addition, the melting trace and vein pattern can be seen clearly in Figure 6b. The plastically deformed Ti particles on the fracture surface indicate that the energy of the shear band has been effectively absorbed by these ductile Ti particles. This suggests that the dispersed Ti particles can limit the propagation of shear banding.

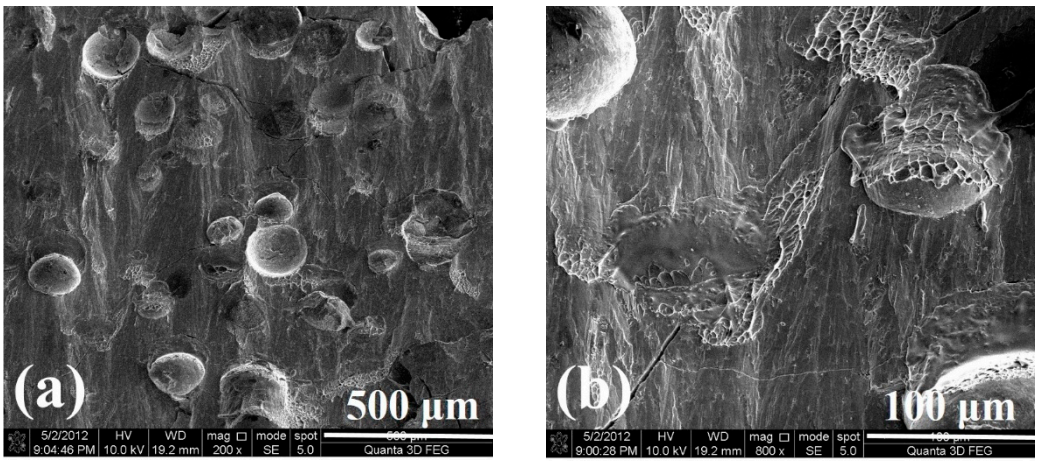

Figure 6. Scanning electron microscopy (SEM) micrographs of (**a**) fracture surface of specimen after compression test for the $Mg_{60}Zn_{35}Ca_5$ BMGC containing 50 vol % Ti particles with sizes of 75–105 μm; (**b**) Enlarged image of Figure 6 (**a**), some areas display vein pattern mixed with melting trace around Ti particles.

4. Conclusions

In summary, Mg-based BMG composites with different particle sizes and the volume fraction of spherical Ti particles were successfully developed in this study. The results show that *ex-situ*-added Ti particles exhibit a positive effect on strengthening $Mg_{60}Zn_{35}Ca_5$-based BMGCs. In addition, both the fracture toughness and the compression failure strain show a similar trend, increasing with a decreasing mean free path of the shear band (the interspacing of Ti particles). However, the performance of these Mg-based BMGCs is strongly dependent on the adhesion ability between the interface of the Ti particle/amorphous matrix. Overall, the dispersion of Ti particles in $Mg_{60}Zn_{35}Ca_5$ BMG alloys is considered to be a possible way in enhancing their plasticity as well as yield strength.

Acknowledgments: The authors would like to grateful acknowledge the sponsorship from Ministry of Science and Technology, Taiwan, under the Contract No. NSC101-2221-E-008-043-MY3, MOST103-2120-M-110-004, and MOST103-2221-E-008-028-MY3.

Author Contributions: Pei Chun Wong and Jason Shian-Ching Jang conceived and designed the experiments; Pei Chun Wong, Tsung Hsiung Lee and Pei Hua Tsai performed the experiments; Pei Chun Wong, Tsung Hsiung Lee and Pei Hua Tsai analyzed the data; Pei Chun Wong, Cheng Kung Cheng, Chuan Li, Jason Shian-Ching Jang and J. C. Huang contributed reagents, materials and analysis tools; Pei Chun Wong, Pei Hua Tsai and Jason Shian-Ching Jang wrote the paper.

Conflicts of Interest: The authors declare no conflict of interest.

References

1. Mordin, M.; Frankel, V.H. *Basic Biomechanics of the Musculoskeletal System*, 4th ed.; Lippincott Williams & Willkin: Philadelphia, PA, USA, 2012.
2. Zberg, B.; Uggowitzer, P.J.; Loffler, J.F. MgZnCa glasses without clinically observable hydrogen evolution for biodegradable implants. *Nat. Mater.* **2009**, *8*, 887–891. [CrossRef] [PubMed]
3. Gu, X.N.; Zheng, Y.F.; Zhong, S.P.; Xi, T.F.; Wang, J.Q.; Wang, W.H. Corrosion of, and cellular response to Mg-Zn-Ca bulk metallic glasses. *Biomaterials* **2010**, *31*, 1093–1103. [CrossRef] [PubMed]
4. Li, Q.F.; Weng, H.R.; Suo, Z.Y.; Ren, Y.L.; Yuan, X.G.; Qiu, K.Q. Microstructure and mechanical properties of bulk Mg-Zn-Ca amorphous alloy and amorphous matrix composites. *Mater. Sci. Eng. A* **2008**, *487*, 301–308. [CrossRef]
5. Zhao, Y.Y.; Ma, E.; Xu, J. Reliability of compressive fracture strength of Mg-Zn-Ca bilk metallic glass: Flaw sensitivity and Weibull statistics. *Scr. Mater.* **2009**, *58*, 496–499. [CrossRef]
6. Zberg, B.; Arata, E.R.; Uggowitzer, P.J.; Loffler, J.F. Tensile properties of glassy MgZnCa wires and reliability analysis using Weibull statistics. *Acta Mater.* **2009**, *57*, 3223–3231. [CrossRef]
7. Jang, J.S.C.; Li, T.H.; Jian, S.R.; Huang, J.C.; Nieh, T.G. Effects of characteristics of Mo dispersions on the plasticity of Mg-based bulk metallic glass composites. *Intermetallics* **2011**, *19*, 738–743. [CrossRef]
8. Hsieh, P.J.; Yang, L.C.; Su, H.C.; Lu, C.C.; Jang, J.S.C. Improvement of mechanical properties in MgCuYNdAg bulk metallic glasses with adding Mo particles. *J. Alloy. Compd.* **2010**, *504*, 98–101. [CrossRef]
9. Jang, J.S.C.; Chang, Y.S.; Li, T.H.; Hsieh, P.J.; Huang, J.C.; Tsao, C.Y. Plasticity enhancement of Mg58Cu28.5Gd11Ag2.5 based bulk metallic glass composites dispersion strengthened by Ti particles. *J. Alloy. Compd.* **2010**, *504*, 102–105. [CrossRef]
10. Kinaka, M.; Kato, H.; Hasegawa, M.; Inoue, A. High specific strength Mg-based metallic glass matrix composite highly ductilized by Ti dispersoid. *Mater. Sci. Eng. A* **2008**, *494*, 299–303. [CrossRef]
11. Shanthi, M.; Gupta, M.; Jarfors, A.E.W.; Tan, M.J. Synthesis characterization and mechanical properties of nano alumina particulate reinforced magnesium based bulk metallic glass composites. *Mater. Sci. Eng. A* **2011**, *528*, 6045–6050. [CrossRef]
12. Xu, Y.K.; Ma, H.; Xu, J.; Ma, E. Mg-based bulk metallic glass composites with plasticity and gigapascal strength. *Acta Mater.* **2005**, *53*, 1857–1866. [CrossRef]
13. Jang, J.S.C.; Jian, S.R.; Li, T.H.; Huang, J.C.; Tsao, C.Y.; Liu, C.T. Structural and mechanical characterizations of ductile Fe particles-reinforced Mg-based bulk metallic glass composites. *J. Alloy. Compd.* **2009**, *485*, 290–294. [CrossRef]

14. Jang, J.S.C.; Ciou, J.Y.; Li, T.H.; Huang, J.C.; Nieh, T.G. Dispersion toughening of Mg-based bulk metallic glass reinforced with porous Mo particles. *Intermetallics* **2010**, *18*, 451–458. [CrossRef]
15. Jang, J.S.C.; Li, J.B.; Lee, S.L.; Chang, Y.S.; Jian, S.R.; Huang, J.C.; Nieh, T.G. Prominent plasticity of Mg-based bulk metallic glass composites by *ex-situ* spherical Ti particles. *Intermetallics* **2012**, *30*, 25–29. [CrossRef]
16. Wang, J.F.; Huang, S.; Wei, Y.Y.; Guo, S.F.; Pan, F.S. Enhanced mechanical properties and corrosion resistance of a Mg-Zn-Ca bulk metallic glass composite by Fe particle addition. *Mater. Lett.* **2013**, *91*, 311–314. [CrossRef]
17. Wang, J.F.; Huang, S.; Li, Y.; Wei, Y.Y.; Guo, S.F.; Pan, F.S. Ultrahigh strength MgZnCa eutectic alloy/Fe particle composites with excellent plasticity. *Mater. Lett.* **2014**, *137*, 139–142. [CrossRef]
18. Xi, X.K.; Zhao, D.Q.; Pan, M.X.; Wang, W.H.; Wu, Y.; Lewandowski, J.J. Fracture of Brittle Metallic Glasses: Brittleness or Plasticity. *Phys. Rev. Lett.* **2005**, *94*. [CrossRef] [PubMed]
19. Meyers, M.A.; Chawla, K.K. *Mechanical Behavior of Materials*; Cambridge University Press: Cambridge, UK, 2009.